LANGMUIR

Article

pubs.acs.org/Langmuir

Stable, Fluorescent Polymethylmethacrylate Particles for the Long-Term Observation of Slow Colloidal Dynamics

Thomas E. Kodger,[†,§] Peter J. Lu,[†,§] G. Reid Wiseman,[‡] and David A. Weitz*[,†]

[†]Department of Physics and SEAS, Harvard University, Cambridge, Massachusetts 02138, United States

[‡]International Space Station, Low Earth Orbit, and NASA Johnson Space Center, Houston, Texas 77058, United States

ABSTRACT: Suspensions of solid micron-scale colloidal particles in liquid solvents are a foundational model system used to explore a wide range of phase transitions, including crystallization, gelation, spinodal decomposition, and the glass transition. One of the most commonly used systems for these investigations is the fluorescent spherical particles of polymethylmethacrylate (PMMA) suspended in a mixture of nonpolar solvents that match the density and the refractive index of the particles to minimize sedimentation and scattering. However, the particles can swell in these solvents, changing their size and density, and may leak the fluorescent dye over days to weeks; this constrains the exploration of slow and kinetically limited processes, such as near-boundary phase separation or the glass transition. In this paper, we produce PMMA colloidal particles that employ polymerizable and photostable cyanine-based fluorescent monomers spanning the range of visible wavelengths and a polymeric stabilizer prepared from polydimethylsiloxane, PDMS-*graft*-PMMA. Using microcalorimetry, we characterize the thermodynamics of an accelerated equilibration process for these dispersions in the buoyancy- and refractive-index-matching solvents. We use confocal differential dynamic microscopy to demonstrate that they behave as hard spheres. The suspended particles are stable for months to years, maintaining fixed particle size and density, and do not leak dye. Thus, these particles enable longer term experiments than may have been possible earlier; we demonstrate this by observing spinodal decomposition in a mixture of these particles with a depletant polymer in the microgravity environment of the International Space Station. Using fluorescence microscopy, we observe coarsening over several months and measure the growth of the characteristic length scale to be a fraction of a picometer per second; this rate is among the slowest observed in a phase-separating system. Our protocols should facilitate the synthesis of a variety of particles.

INTRODUCTION

Colloidal particles have long been an effective model system for studying phase behavior.[1−4] With sizes ranging from tens of nanometers to several microns, colloids are driven by thermodynamics, and they are easily probed with common laboratory optical techniques. Early studies used light scattering and photography to characterize bulk colloidal phase transitions, such as crystallization[3,5] and glass formation;[6] subsequent studies used microscopy to gain a more detailed view. More recently, confocal microscopy has been used to elucidate microscopic explanations for macroscopic phenomena, such as the dynamical heterogeneity underlying the glass transition,[7] by giving a detailed view of the three-dimensional (3D) positions and motions of individual particles.[8−12]

The model suspensions used in these studies, comprising solid colloidal particles in liquid solvents, have several particular properties. The particles and solvents must share similar refractive indices n to minimize scattering at the particle−fluid interfaces and allow light to probe the particles deep in the sample bulk, and a similar density ρ to limit sedimentation. Furthermore, microscopy requires a contrast mechanism to distinguish the particles from the solvent; most commonly, a fluorescent dye is added to the particles.[13−15] A well-established colloidal model system is polymethylmethacrylate (PMMA), which was used to elucidate the hard-sphere crystallization in the pioneering work 30 years ago.[3,16] Colloidal PMMA particles are readily suspended in the mixtures of organic solvents that match n and ρ; moreover, a wide range of fluorescent dyes can be incorporated.

Nonetheless, existing PMMA suspensions have some practical limitations. In general, solvent mixtures that match n and ρ contain components that are good solvents for PMMA, which tend to swell the particles;[17] this changes their size and density and allows fluorescent dyes that are not chemically linked to the PMMA chains themselves to leach out of the particles. Consequently, suspensions of the dyed particles may have a volume fraction ϕ and a particle radius r that remain measurably unchanged for only a few days to weeks;[18] moreover, the particles tend to fade in brightness as their dye leaks into the surrounding solvent. Finally, many common dyes that have been incorporated into the PMMA particles are charged, imparting a Coulombic repulsion to the particles, which softens their interparticle potential away from the oft-desired hard-sphere interaction.[19] These drawbacks constrain the applicability and generality of the PMMA particle system, in particular, limiting the exploration of phenomena that occur on time scales longer than a few days. Such slow processes are of a significant present interest to scientists in several fields,

Received: March 14, 2017
Revised: May 15, 2017
Published: May 31, 2017

DOI: 10.1021/acs.langmuir.7b00852
Langmuir 2017, 33, 6382−6389

including the glass transition,[20,21] gelation,[22−25] crystallization,[26,27] and phase separation[28] near a phase boundary or a critical point.

In this paper, we describe and characterize a substantially improved PMMA particle system comprising monodisperse, fluorescent particles that do not bleach, leak dye, or appear to carry any significant Coulombic charge and remain stable for at least several months. Our particles incorporate two novel syntheses: fluorescent dyes covering the range of commonly used visible wavelengths linked covalently to methylmethacrylate (MMA) monomers, which are incorporated into the particle bulk during polymerization and therefore do not leak; and a stabilization layer based on polydimethylsiloxane (PDMS) that replaces the hard-to-synthesize polyhydroxystearic acid (PHSA).[13,16,29−31] Our simplified single-flask syntheses require only chemical components that are readily available commercially. We characterize the thermodynamics of a "heat-shock" process that accelerates significantly the equilibration of particles in the final index- and density-matching solvent mixtures.[32] Furthermore, we present a method to fabricate chemically resistant sample chambers with soft lithography and demonstrate that our particles subsequently behave like hard spheres and remain stable for many months on earth and aboard the International Space Station (ISS). Finally, we use these particles to investigate extremely slow phase separation in microgravity, observing continuously for months a spinodal decomposition coarsening rate of less than a picometer per second, among the slowest ever observed.

SYNTHESIS

PDMS Stabilizer. We polymerize the MMA monomers to form spherical colloids in the presence of small polymer brushes, which form a thin steric barrier layer preventing the particles from aggregating because of van der Waals attractions,[15,16] as shown in the schematic of Figure 1a−c.

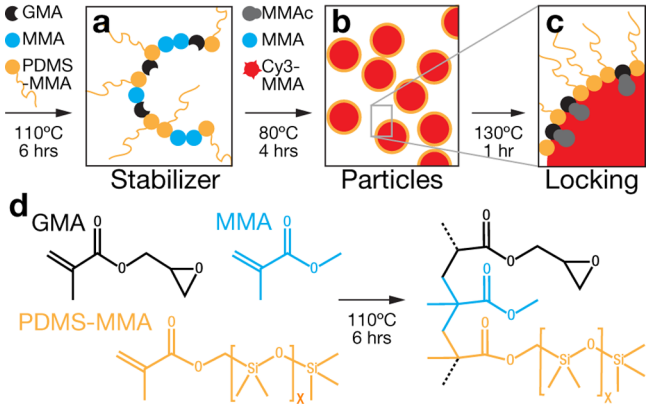

Figure 1. Synthesis of stabilizer and particles. Schematics of the synthesis of (a) stabilizer and (b) particles, with a (c) final locking stage. (d) Chemical components of the stabilizer.

Traditionally, these stabilizers were synthesized from PHSA, which is no longer available commercially; in response, new syntheses from more basic precursors have been devised,[15,17] with recent work improving PHSA via the controlled polycondensation of hydroxystearic acid (HSA),[31] but these are all complex procedures involving several steps. Therefore, we present a new, single-flask synthesis of a stabilizer based on PDMS, which is a low-cost polymer readily available over a wide range of molecular weights, M_w, at high quality with a narrow distribution,[29,33,34] creating a comb polymer that can be grafted directly onto the surface of PMMA,[16] as shown in the schematic of Figure 1a. We start with two PDMS−monomethacrylate (PDMS−MMA) polymers (Gelest) that we measure using a gel permeation chromatography (Malvern Viscotek) to have M_w values of 5880 and 10 580 and monodispersity values of polydispersity index (PDI) = 1.02 and 1.05, respectively. In a single glass syringe, we combine PDMS−MMA, MMA, glycidyl methacrylate, free-radical initiator azobisisobutyronitrile (AIBN), and toluene and remove the dissolved oxygen by bubbling with argon for 10 min. We connect the syringe with fluorinated ethylene propylene tubing to a 100 mL three-neck flask charged with acetates and a small stir bar, heated in an oil bath to 110 °C with a reflux condenser. We add the syringe contents dropwise at 8 mL/h, allowing the reaction to proceed to completion for an additional 2 h and then cool to room temperature. We generate a wide variety of brush stabilizer sizes by varying the monomer stoichiometry, as shown in Table 1.

Table 1. Composition of Particle Stabilizers[a]

stabilizer	PDMS (mmol)	AIBN (mmol)	M_w	PDI
STAB1a	10.0 g (2)	85 mg (0.5)	16 840	1.51
STAB1b	10.0 g (2)	85 mg (0.5)	23 690	1.53
STAB2	10.0 g[b] (1)	85 mg (0.5)		
STAB3	5.0 g (1)	85 mg (0.5)		
STAB4	10.0 g (2)	42.4 mg (0.25)		

[a]All reactions include 5.00 g of MMA (50 mmol), 110 mg of GMA (0.77 mmol), 7.75 mL of toluene in the syringe, 4.4 mL of ethyl acetate, and 2.2 mL of butyl acetate in the flask. [b]Denotes 10 kDa PDMS. STAB1a and STAB1b are repeats of the same recipe.

Monomer-Linked Fluorescent Dye. Existing PMMA particles used in microscopy often use a physical mechanism to trap the fluorescent dye in the polymer matrix, typically during polymerization, without any chemical linkage. When these particles are suspended in solvent mixtures that match n and ρ, one or more of the solvent components are usually a good solvent for PMMA, preferentially migrating around the PMMA chains; this selective migration slowly swells the particles and increases their size, causing the dye to leak out, which in turn decreases the imaging contrast significantly over time. Moreover, heating dyed particles to accelerate the solvent equilibration drives out the dye more quickly; consequently, typical sample preparation procedures let the dyed particles equilibrate in the swelling solvents for months at room temperature, without heating. Under these conditions, particles do not appear to ever equilibrate fully; instead, the swelling continuously increases the particle size and ρ and causes them to leak the dye and fade. Consequently, these particles have stable properties for only a few days, limiting the observation of slow colloidal processes, such as glass dynamics, phase separation, gelation, and crystallization, which may occur over far longer time scales. Finally, many fluorescent dyes used commonly for colloids[13] are hydrophilic and possess a net charge, leading to size polydispersity during particle synthesis and unwanted electrostatic interactions, respectively.

To overcome these problems, we synthesize new dyes based on common lipophilic cyanine fluorophores[25,35,36] that are known to have excellent photostability, quantum efficiencies, a wide range of excitation wavelengths, and do not carry a

DOI: 10.1021/acs.langmuir.7b00852
Langmuir 2017, 33, 6382−6389

significant Coulombic charge. We link in three steps the free radical polymerizable analogs of DiO, DiI, and DiD (Cy2, Cy3, and Cy5 dyes, respectively) covalently to the MMA monomers, yielding the three new molecules Cy2-MMA, Cy3-MMA, and Cy5-MMA, adapting protocols from several published sources;[37−39] these molecules are then polymerized into the PMMA chains during particle synthesis, unlike previous strategies which physically trap the non-reactive dyes inside of the particle[35,36] and are thus prone to leakage.

We present the synthesis schematic of Cy2-MMA in Figure 2a. Recipe **3**: 2-methylbenzoxazole (**1**, 10 mmol) and 4-bromomethyl phenyl acetic acid (**2**, 10 mmol) were added to 1,2-dichlorobenzene ($BzCl_2$, 50 mL) and heated to 110 °C for 12 h. The product was cooled to room temperature, filtered, and washed with acetonitrile (30 mL, 3×) to obtain the yellow salt (2.72 g, 78%). Recipe **5**: ethyl-2-methylbenzoxazolium iodide (**4**, 5 mmol) and diphenylformamide (6 mmol) were added to acetic anhydride (Ac_2O, 15 mL) and heated to 130 °C for 1 h. **Cy2-MMA**: to the uncleaned reaction of **5**, pyridine (15 mL) and **3** (6 mmol) were added and stirred for 24 h at 25 °C. The solvent was removed under reduced pressure, and the product was redissolved in chloroform (50 mL), dehydrated with sodium sulfate, filtered, and fully dried under reduced pressure. This intermediate (1.3 mmol) was then esterified; chloroform ($CHCl_3$, 40 mL), 4-(dimethylamino)pyridine (DMAP, 0.4 mmol), and 2-hydroxyethyl methacrylate (HEMA, 4.5 mmol) were added to the flask, followed by *N*,*N*-dicyclohexylcarbodiimide (DCC, 2 mmol). This final reaction proceeded at 25 °C for 24 h and then it was filtered and washed with water (200 mL), and the organic phase was dried and removed under reduced pressure to yield a bright yellow solid Cy2-MMA (0.53 g) with peak excitation at 488 nm and peak emission at 520 nm.

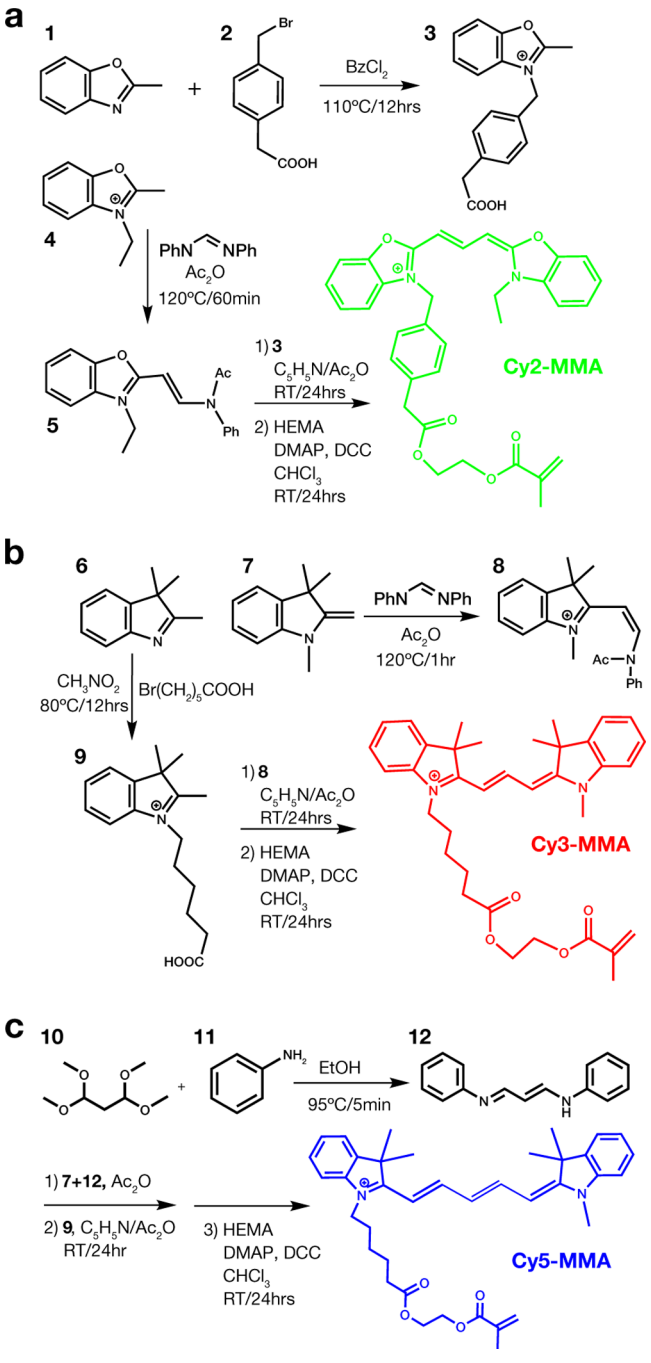

Figure 2. Synthesis schemes of (a) Cy2-MMA, (b) Cy3-MMA, and (c) Cy5-MMA.

We present the synthesis schematic of Cy3-MMA in Figure 2b. Recipe **9**: 2,3,3-trimethylindolenine (**6**, 33 mmol) and 6-bromohexanoic acid (33 mmol) were added to nitromethane (20 mL) and heated to 80 °C for 24 h. The product was precipitated into diethyl ether (150 mL), filtered, and then washed with diethyl ether (50 mL, 2×) to yield a light red powder (4.84 g, 42%). Recipe **8**: 1,3,3-trimethyl-2-methyleneindoline (7, 5 mmol) and diphenylformamide (6 mmol) were added to Ac_2O (15 mL) and heated to 130 °C for 1 h. **Cy3-MMA**: to the uncleaned reaction of **8**, pyridine (15 mL) and **9** (6 mmol) were added and stirred for 24 h at 25 °C. The solvent was removed under reduced pressure, and the product was redissolved in chloroform (50 mL), dried with sodium sulfate, filtered, and fully dried under reduced pressure. This intermediate (2.9 mmol) was then esterified; chloroform (40 mL), DMAP (1.1 mmol), and HEMA (12 mmol) were added, followed by DCC (4.4 mmol). This final reaction proceeded at 25 °C for 24 h and then it was filtered and washed with water (200 mL), and the organic phase was dried and removed under reduced pressure to yield a bright red solid Cy3-MMA (1.18 g) with peak excitation at 562 nm and peak emission at 585 nm.

We present the synthesis schematic of Cy5-MMA in Figure 2c. Recipe **12**: 1,1,3,3-tetramethoxypropane (**10**, 115 mmol), aniline (**11**, 230 mmol), and 25 mL of ethanol were heated to 95 °C for 5 min.[39] The reaction was cooled, and concentrated HCl (25 mL) was added dropwise. After the addition of ice, the precipitate was filtered and washed with water, followed by diethyl ether and fully dried in vacuum. The recipes **12** (6 mmol) and 7 (6 mmol) were added to Ac_2O (10 mL) and acetic acid (10 mL), and the mixture was heated to 120 °C for 30 min. This intermediate was cooled, and acetic acid was removed under vacuum. Then, pyridine (15 mL) and **9** (6 mmol) were added and allowed to react for 24 h at room temperature. The product was precipitated in diethyl ether (50 mL, 3×) and fully dried. This intermediate (∼4.1 mmol) was then esterified; chloroform (40 mL), DMAP (1.1 mmol), and HEMA (12 mmol) were added, followed by DCC (4.4 mmol). This final reaction proceeded at 25 °C for 24 h and then it was filtered and washed with water (200 mL), and the organic phase was dried and removed under reduced pressure to yield a bright purple solid Cy5-MMA (2.12 g) with peak excitation at 640 nm and peak emission at 663 nm.

DOI: 10.1021/acs.langmuir.7b00852
Langmuir 2017, 33, 6382−6389

Linking dye molecules to MMA may induce electronic structure changes, potentially affecting interactions with light. To investigate this possibility, we collect the absorption and fluorescence spectra of solutions of DiI, a commercially available lipophilic form of Cy3, and our Cy3-MMA dissolved in the same solvent. The spectra are nearly identical, with emission and absorption peaks shifted by just a few nanometers, as shown in Figure 3a,b.

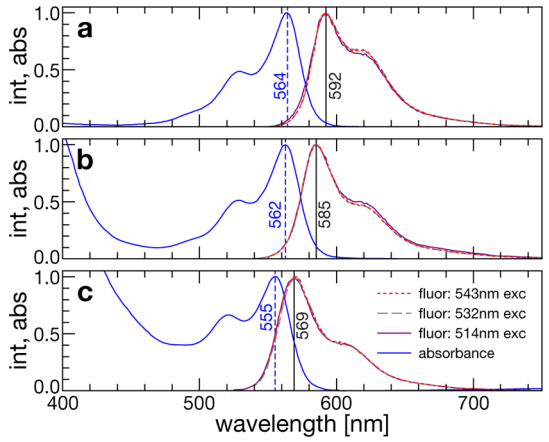

Figure 3. Fluorescence spectra, with excitation (blue) and emission (black) peaks marked, of (a) free DiI fluorophore in solution, (b) Cy3-MMA in solution, and (c) PMMA particles with integral polymerized Cy3-MMA.

Stabilized, Fluorescent PMMA Particles. We synthesize PMMA particles[16] by combining our new PDMS−MMA brush stabilizer, our new Cy3-MMA dye, MMA monomer, methacrylic acid (MAAc), AIBN, and 1-octanethiol in a solvent mixture of hexane and dodecane. We stir these components in a single 200 mL round-bottom flask fitted with a reflux condenser in an oil bath at 80 °C for 3 h; we set the air−reaction mixture interface and the air−oil bath interface at the same height to minimize particle aggregation at the boiling interface. To chemically lock the stabilizer onto the surface of the particles, we remove the reflux condenser, transfer the flask to a silicone oil bath at 130 °C, add 50 μL of 2-dimethylaminoethanol, and mix for 1 h, adding an equal volume of dodecane to replace the evaporating hexane, thereby keeping constant the particle density in the flask. We then cool the reaction vessel to room temperature and resuspend the colloids in *cis*-decalin via centrifugation, for long-term storage.

CHARACTERIZATION

Particle Size. Changing the initial volume fraction of the MMA monomer produces a wide range of particle sizes; using SEM, we measure $0.25 < r < 2$ μm, as shown in Figure 4 and described in Table 2. In general, our fluorescent colloids have low size PDI $\equiv \sigma/\overline{r}$ (where $\overline{r}$ is the average radius and σ is the standard deviation), and the particles crystallize easily; however, small changes in the stabilizer stoichiometry lead to some differences in the $\overline{r}$ and σ of the resulting suspension, as shown in Figure 4a−e. Repeating the same stabilizer stoichiometry, for example, as in STAB1a and STAB1b, can yield differences in $\overline{r}$, as shown in Figure 4a,b; however, with the same stabilizer, $\overline{r}$ can be tuned, as shown in Figure 4f. When greater polydispersity is desired, for example, to study amorphous or glassy phases, our protocol facilitates single batches of more polydisperse colloids;

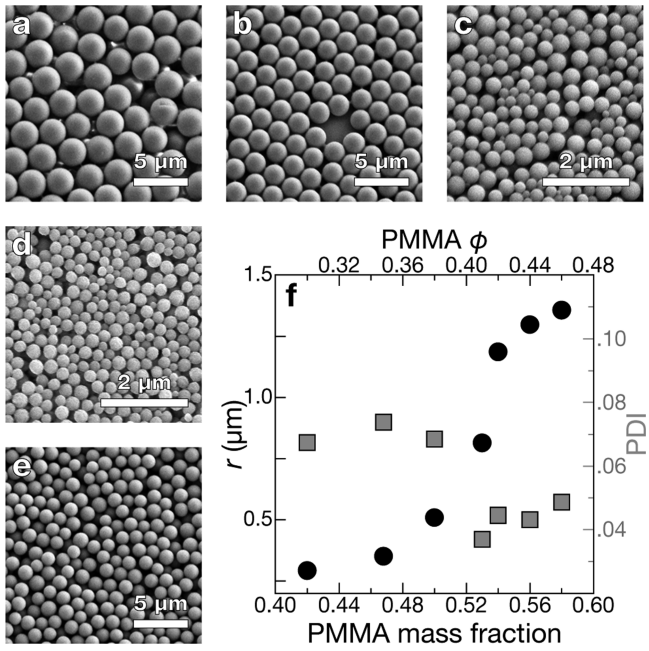

Figure 4. Scanning electron microscopy (SEM) images of particles using recipe 6 in Table 2. (a) STAB1a: $\overline{r}$ = 1.31 μm, PDI = 0.031; (b) STAB1b: $\overline{r}$ = 1.01 μm, PDI = 0.027; (c) STAB2: $\overline{r}$ = 0.14 μm, PDI = 0.20; (d) STAB3: $\overline{r}$ = 0.13 μm, PDI = 0.178; (e) STAB4, $\overline{r}$ = 0.62 μm, PDI = 0.07. (f) Particle $\overline{r}$ (black circles) and σ (gray squares) determined from SEM images for recipes 1−7 from Table 2.

Table 2. Recipes for Colloidal Particles[a]

recipe	hexane	dodecane	PMMA-ϕ	$\overline{r}$ (μm)	PDI (N)
1	25.7	14.7	29	0.292	0.067 (1272)
2	19.3	11.0	34.8	0.350	0.073 (637)
3	17.47	9.97	38	0.501	0.068 (1690)
4	14.67	8.36	41	0.815	0.036 (3301)
5	13.95	7.95	42	1.18	0.044 (1430)
6	12.85	7.32	44	1.30	0.043 (1255)
7	11.77	6.70	46	1.36	0.048 (2819)
8	10.77	6.14	48	2.02	0.35 (2900)

[a]In all cases, several ratios are kept constant: hexane/dodecane, 2:1 by volume; 1-octanethiol/MMA monomer, 1:200 by mass; MAAc/MMA, 1:50 by mass. All recipes use 1.51 ± 0.02 g of stabilizer; 30.1 ± 0.1 g of MMA, 0.6 g of MAAc, 0.242 ± 0.04 g of AIBN, and 0.15 g of 1-octanethiol. The column PMMA-ϕ is the assumed volume fraction of PMMA after polymerization, and N is the number of particle counted. STAB1a is used for all methods.

for example, the stabilizer STAB4 leads consistently to colloidal suspensions with PDI = 0.07 compared to the minimum polydispersity required to prevent hard-sphere crystallization,[40] as shown in Figure 4e.

Heat Shock and Swelling. The fluorescent PMMA particles stored in alkanes, such as *cis*-decalin or dodecane, remain stable for at least several years; however, in the solvent mixtures required to match n and ρ, the particles swell slowly and continuously at room temperature. To accelerate the kinetics of this solvent equilibration, we heat[32] a suspension of our colloidal particles in an 18:22:60 (by mass) mixture of *cis*-decalin/tetralin/tetrachloroethylene, which matches n and ρ of the particles upon cooling to room temperature.[41] In traditional particles with physically trapped dyes, this heating usually causes significant dye leakage from particles into the solvent; by

DOI: 10.1021/acs.langmuir.7b00852
Langmuir 2017, 33, 6382−6389

contrast, because the dyes in our particles are covalently linked, we observe no such dye leakage in our samples upon heating. The optimal parameters for this process, however, are not known; therefore, to investigate the thermodynamics of this "heat-shock" process, we use solution microcalorimetry (NanoDSC, TA Instruments) to probe the isothermal swelling of the colloidal suspension at different temperatures. We observe that the equilibration time t_{eq}, the time when there is zero heat flow between the particles and the solvent, decreases with an increasing temperature, as shown in Figure 5a.

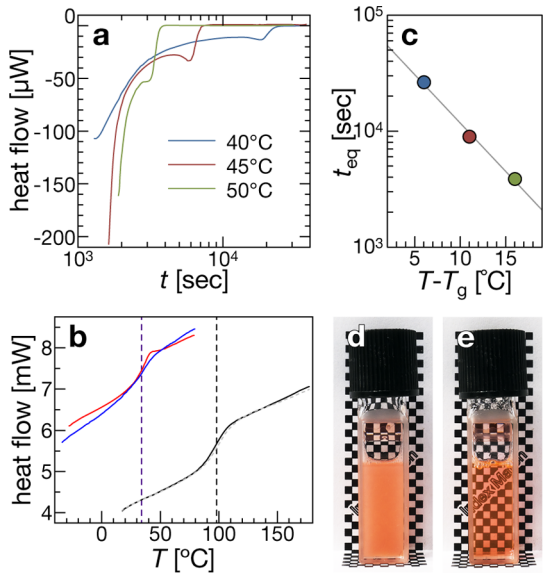

Figure 5. (a–c) Differential scanning calorimetry (DSC) for PMMA particles. (a) Heat flux from isothermal DSC of a PMMA particle suspension equilibrating in a solvent mixture that matches n and ρ at 40, 45, and 50 °C. (b) Heat flow for one heating and cooling cycle of the PMMA particles in suspension after heat shock, upper red and blue curves, T_g = 34 °C, and of the dried PMMA particles, lower gray and black curves, T_g = 98 °C; the dashed vertical lines represent T_g for each sample. (c) Equilibration time t_{eq} as a function of temperature difference from the glass transition temperature T_g = 34 °C. (d,e) Macroscopic images of a particle suspension (d) before and (e) after heat shock at 50 °C for 1 h; vial is 1 cm across.

After equilibration, we measure the colloidal glass transition temperature T_g of the particles by temperature cycling from −20 to 80 °C; the resulting T_g = 34 °C represents a substantial drop from the near-literature value obtained for the dried PMMA particles, 98 °C, as shown in Figure 5b. From this drop in T_g, we can estimate the mass fraction of the particle that is TCE, which is assumed to be the primary plasticizer in the mixture, using the empirical relation,[42] $T_g = T_{g1}w_1 + T_{g2}w_2 + Kw_1w_2$, where T_{g1} = 371 K and T_{g2} = 143 K are the glass transition temperatures of the non-plasticized PMMA and the plasticizer TCE,[43] w_1 and w_2 are the mass fractions of PMMA and TCE, respectively, and K = −130 ± 50 K is an experimentally determined constant for the pure PMMA.[44] We calculate w_2 = 0.20 ± 0.03, which only depends weakly on the magnitude of K, not directly determined for this PMMA polymer, and that the equilibrated PMMA colloids are ≈15 vol % plasticizer, corresponding to a slight increase in r by a few percent; for room temperature experiments, only slightly below T_g = 34 °C, these particles might be considered to be highly viscous droplets and not entirely solid. Finally, we explore the relationship between T_g and t_{eq} for different temperatures; we find $t_{eq} \propto e^{(T-T_g)}$, analogous to the relation $\eta \propto e^{(T-T_g)}$ known for polymer glasses, as shown in Figure 5c.

On the basis of these calorimetric results, we apply a "heat shock" by placing a $\phi \approx 0.20$ colloidal suspension in an oven at 50 °C and equilibrating for >1 h. Before the heat shock, the suspension is turbid, as shown in Figure 5d. After the heat shock and cooling to room temperature at 22 °C, the suspension becomes well-matched in both n and ρ, as shown in Figure 5e. This protocol does not lead to appreciable fading or degradation of the dye, which we observe at equilibration temperatures above 90 °C. To quantify how heating might affect the optical response of the fluorescent dye, we collect the spectra of the heat-shocked particles in the solvent mixture and observe that the Cy3-MMA red particles are only slightly blue-shifted relative to the free dye in solution, as shown in Figure 3c.

Solvent-Resistant Sample Chambers for Microscopy. Colloidal suspensions are commonly sealed in glass capillaries for imaging with confocal microscopy. However, these borosilicate capillaries with $n \approx 1.47$ often do not match the colloidal suspensions, which we measure in our samples to be n = 1.505; furthermore, the capillary wall thickness is typically around 200 μm, significantly exceeding the 170 μm thickness of the no. 1.5 coverslips with n = 1.515, for which the high-magnification oil-immersion microscope objectives are designed. Consequently, the confocal images collected deep within a sample loaded into a capillary tend to degrade, losing contrast and intensity, owing to spherical aberration. To improve these images, we create new sample chambers by casting chemically resistant epoxy from a mold created with soft lithography techniques and bonded to a no. 1.5 microscope coverslip to permit proper imaging conditions. We pattern a photographic template onto a silicon wafer and create a PDMS stamp,[45,46] as shown in Figure 6a–c; the PDMS stamp is the reverse of the final chamber, as shown in Figure 6c. We press the stamp against a microscope slide, and flow in a small volume of 5 min epoxy, remove the stamp after 12 min, and

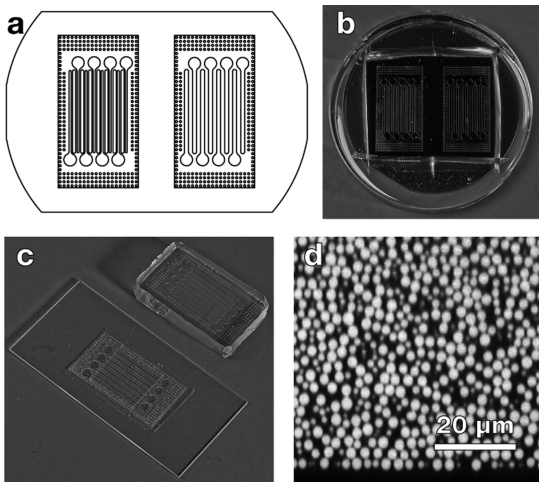

Figure 6. Fabrication of solvent-resistant sample chambers. (a) CAD drawing of photolithographic mask; the mask outlines two stamps each with eight inlets (circles) and eight channels where the colloidal suspensions are loaded. (b) SU8 template on a silicon wafer, created from the mask using soft lithography. (c) Above right, a PDMS stamp from the master; below left, an empty final flow chamber. (d) Single $\hat{x}$–$\hat{z}$ confocal slice of a dense sediment, with coverslip at the bottom.

DOI: 10.1021/acs.langmuir.7b00852
Langmuir 2017, 33, 6382–6389

immediately press in place an 18 mm square no. 1.5 coverslip; to fully cure the epoxy, we heat the sample chamber overnight at 65 °C. We load the colloidal samples into the chambers with glass pipettes and seal with 5 min epoxy; when sealed properly, our samples do not leak for months to years. Moreover, by using a proper coverslip, we minimize spherical aberration; particles remain bright and clear even deep into dense colloidal sediments with $\phi > 0.5$, as shown in the $\hat{x}-\hat{z}$ confocal image (Leica SP5) in Figure 6d.

Hard-Sphere Behavior with Confocal Differential Dynamic Microscopy. To characterize the size of our particles and the degree to which they behave as hard spheres, we use confocal differential dynamic microscopy (ConDDM)[41] to probe suspensions of heat-shocked particles in the stamped sample chambers. We measure $\tau(q)$ of a dilute suspension with $\phi < 0.01$ and extract the diffusion constant from the high-q limit; we find from the Stokes−Einstein equation using η = 1.288 mPa s that r = 0.290 μm, as shown in Figure 7a. We

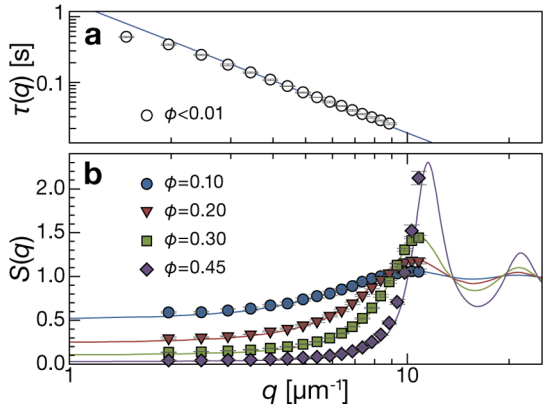

Figure 7. (a) $\tau(q)$ from ConDDM of dilute $\phi < 0.01$ suspension; fitting of high-q data to $1/q^2$ yields r = 0.290 μm. The error bars are from an average over 10 000 frames. (b) $S(q)$ from ConDDM from several suspensions, with ϕ = 0.10, 0.20, 0.30, and 0.45 (symbols) and fit to the Percus−Yevick model for a = 0.293 μm.

measure $S(q)$ for suspensions of the same particles over a wide range of ϕ, as shown with symbols in Figure 7b; by calculating $S(q)$ for hard-sphere suspensions in the Percus−Yevick approximation at the same densities as the experimental samples, we fit the radius and show that it is consistent with r = 0.293 μm. This is in an excellent agreement with the size derived from the $\tau(q)$ measurement. Together, these data demonstrate that our particle systems have no significant interparticle Coulombic repulsion[41] and behave as hard spheres as well as, or better than, existing systems of colloids stabilized with polymer brushes.

Slow Phase Separation. The stability of our particle system allows us to explore with microscopy slow phenomena that may progress over weeks to months, such as near-critical phase separation, slow multicomponent crystallization, and dynamics approaching the glass transition. On these time scales, however, even slight sedimentation may affect the observed phase behavior. On earth, careful sample preparation and reasonable temperature control ±0.1 °C allow us to match the densities of colloid and solvent mixture to within a few parts in ten thousand;[10,22,23] to further reduce sedimentation by several orders of magnitude, we observe our colloidal suspensions aboard the ISS, where the effective buoyancy difference, relative to a regular non-density-matched colloidal suspension on earth, approaches about one in a billion—essentially a nanogravity regime.

To explore slow phase behavior in this environment, we add a linear polystyrene depletant to a properly heat-shocked colloidal suspension, which causes the sample to undergo spinodal decomposition into a colloid-rich liquid-like phase and a colloid-poor gas-like phase.[28] We seal the sample in a quartz sample chamber, fly it to the ISS as part of the ACE-M2 experiment, and observe the phase separation over time with a 10× air objective in a modified fluorescence microscope (NASA Light Microscopy Module); the sample coarsens slowly, with no significant fading, for several months, as seen in the images in Figure 8a−c. We quantify this coarsening by

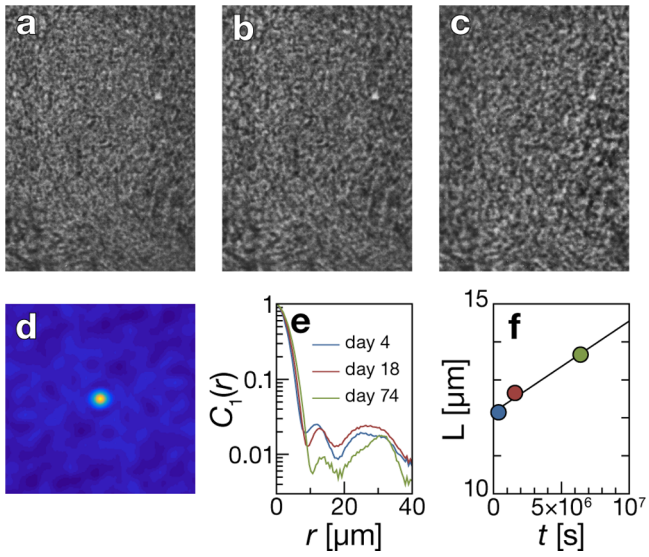

Figure 8. Phase-separating colloid-polymer sample in microgravity imaged using wide-field fluorescence microscopy with a 10× objective, (a) 4, (b) 18, and (c) 74 days after initial mixing. The sample coarsens without fading or loss of contrast due to dye degradation or leakage. (d) 2D intensity autocorrelation extending ±50 microns in $\hat{x}$ and $\hat{y}$ real-space dimensions. (e) 1D azimuthal averages at the times shown in (a−c). (f) Position of the first peak, corresponding to a characteristic length scale L, grows at 0.24 pm/s.

calculating the 2D intensity−intensity autocorrelation function for each image, as shown in Figure 8d; we average this azimuthally to generate the 1D scalar intensity autocorrelation, $C_1(r)$, shown for the three images in Figure 8e. We define the first peak after the main decay to be a characteristic length scale L, which grows monotonically, as shown in Figure 8f. Strikingly, we measure L to grow at a very slow rate of 0.24 pm/s, among the slowest measured in any system.

CONCLUSIONS

These data demonstrate how our particles make possible new experiments that require stable, long-time observations, and the ability to resolve each particle individually with microscopy, thereby improving the quality, consistency, and reproducibility of the colloidal experiments. These particles should enable other long-duration observation of thermodynamic transitions close to phase boundaries, such as slow or binary crystallization and near-critical spinodal or binodal decomposition; or kinetic processes, such as the approach to the glass transition or gelation line. Beyond these traditional applications, the covalent linkage of dye within our particles will further expand the

DOI: 10.1021/acs.langmuir.7b00852
Langmuir 2017, 33, 6382−6389

number of suitable solvents where these particles can be suspended; the particles should be useful as tracers in multiphase flow, whereas in the past the presence of a polar solvent tended to extract dye from the particles. Moreover, these particles may be more amenable to post-polymerization transformations, such as stretching to create ellipsoids, without losing their fluorescence. Finally, the simplification of existing protocols to single-flask procedures with readily available materials will expand access to many other users.

AUTHOR INFORMATION

Corresponding Author

*E-mail: weitz@seas.harvard.edu.

ORCID

Peter J. Lu: 0000-0003-1489-5725

David A. Weitz: 0000-0001-6678-5208

Author Contributions

§T.E.K. and P.J.L. contributed equally.

Notes

The authors declare no competing financial interest.

ACKNOWLEDGMENTS

T.E.K. and P.J.L. contributed equally to this work, which was supported by NASA (NNX13AQ48G), the National Science Foundation (DMR-1310266), and the Harvard Materials Research Science and Engineering Center (DMR-1420570). We thank A. Hollingsworth, E. Sloutskin, and E. Weeks for helpful comments on the manuscript.

REFERENCES

(1) Kose, A.; Ozaki, M.; Takano, K.; Kobayashi, Y.; Hachisu, S. Direct observation of ordered latex suspension by metallurgical microscope. *J. Colloid Interface Sci.* **1973**, *44*, 330.

(2) Vrij, A.; Jansen, J. W.; Dhont, J. K. G.; Pathmamanoharan, C.; Kops-Werkhoven, M. M.; Fijnaut, H. M. Light scattering of colloidal dispersions in non-polar solvents at finite concentrations. Silic spheres as model particles for hard-sphere interactions. *Faraday Discuss. Chem. Soc.* **1983**, *76*, 19.

(3) Pusey, P. N.; van Megen, W. Phase behaviour of concentrated suspensions of nearly hard colloidal spheres. *Nature* **1986**, *320*, 340−342.

(4) Lu, P. J.; Weitz, D. A. Colloidal Particles: Crystals, Glasses, and Gels. *Annu. Rev. Condens. Matter Phys.* **2013**, *4*, 217−233.

(5) Zhu, J.; Li, M.; Rogers, R.; Meyer, W.; Ottewill, R. H.; STS-73 Space Shuttle Crew; Russel, W. B.; Chaikin, P. M. Crystallization of hard-sphere colloids in microgravity. *Nature* **1997**, *387*, 883−885.

(6) van Megen, W.; Pusey, P. N. Dynamic light-scattering study of the glass transition in a colloidal suspension. *Phys. Rev. A* **1991**, *43*, 5429.

(7) Weeks, E. R.; Crocker, J. C.; Levitt, A. C.; Schofield, A.; Weitz, D. A. Three-Dimensional Direct Imaging of Structural Relaxation Near the Colloidal Glass Transition. *Science* **2000**, *287*, 627−631.

(8) van Blaaderen, A.; Imhof, A.; Hage, W.; Vrij, A. Three-dimensional imaging of submicrometer colloidal particles in concentrated suspensions using confocal scanning laser microscopy. *Langmuir* **1992**, *8*, 1514.

(9) Crocker, J. C.; Grier, D. G. Methods of Digital Video Microscopy for Colloidal Studies. *J. Colloid Interface Sci.* **1996**, *179*, 298−310.

(10) Lu, P. J.; Sims, P. A.; Oki, H.; Macarthur, J. B.; Weitz, D. A. Target-locking acquisition with real-time confocal (TARC) microscopy. *Opt. Express* **2007**, *15*, 8702−8712.

(11) Schall, P.; Weitz, D. A.; Spaepen, F. Structural Rearrangements That Govern Flow in Colloidal Glasses. *Science* **2007**, *318*, 1895−1899.

(12) Gao, Y.; Kilfoil, M. L. Accurate detection and complete tracking of large populations of features in three dimensions. *Opt. Express* **2009**, *17*, 4685.

(13) Bosma, G.; Pathmamanoharan, C.; de Hoog, E. H. A.; Kegel, W. K.; van Blaaderen, A.; Lekkerkerker, H. N. W. Preparation of Monodisperse, Fluorescent PMMA−Latex Colloids by Dispersion Polymerization. *J. Colloid Interface Sci.* **2002**, *245*, 292−300.

(14) Leunissen, M. E.; Christova, C. G.; Hynninen, A.-P.; Royall, C. P.; Campbell, A. I.; Imhof, A.; Dijkstra, M.; van Roij, R.; van Blaaderen, A. Ionic colloidal crystals of oppositely charged particles. *Nature* **2005**, *437*, 235−240.

(15) Elsesser, M. T.; Hollingsworth, A. D.; Edmond, K. V.; Pine, D. J. Large Core−Shell Poly(methyl methacrylate) Colloidal Clusters: Synthesis, Characterization, and Tracking. *Langmuir* **2011**, *27*, 917−927.

(16) Antl, L.; Goodwin, J. W.; Hill, R. D.; Ottewill, R. H.; Owens, S. M.; Papworth, S.; Waters, J. A. The preparation of poly(methyl methacrylate) latices in non-aqueous media. *Colloids Surf.* **1986**, *17*, 67−78.

(17) Pathmamanoharan, C.; Groot, K.; Dhont, J. K. G. Preparation and characterization of crosslinked PMMA latex particles stabilized by grafted copolymer. *Colloid Polym. Sci.* **1997**, *275*, 897−901.

(18) Poon, W. C. K.; Weeks, E. R.; Royall, C. P. On measuring colloidal volume fractions. *Soft Matter* **2012**, *8*, 21.

(19) Royall, C. P.; Poon, W. C. K.; Weeks, E. R. In search of colloidal hard spheres. *Soft Matter* **2013**, *9*, 17.

(20) Cipelletti, L.; Ramos, L. Slow dynamics in glassy soft matter. *J. Phys.: Condens. Matter* **2005**, *17*, R253.

(21) Lynch, J. M.; Cianci, G. C.; Weeks, E. R. Dynamics and structure of an aging binary colloidal glass. *Phys. Rev. E: Stat., Nonlinear, Soft Matter Phys.* **2008**, *78*, 031410.

(22) Lu, P. J.; Conrad, J. C.; Wyss, H. M.; Schofield, A. B.; Weitz, D. A. Fluids of Clusters in Attractive Colloids. *Phys. Rev. Lett.* **2006**, *96*, 028306.

(23) Lu, P. J.; Zaccarelli, E.; Ciulla, F.; Schofield, A. B.; Sciortino, F.; Weitz, D. A. Gelation of particles with short-range attraction. *Nature* **2008**, *453*, 499−503.

(24) Joshi, Y. M. Dynamics of Colloidal Glasses and Gels. *Annu. Rev. Chem. Biomol. Eng.* **2014**, *5*, 181−202.

(25) Harich, R.; Blythe, T. W.; Hermes, M.; Zaccarelli, E.; Sederman, A. J.; Gladden, L. F.; Poon, W. C. K. Gravitational collapse of depletion-induced colloidal gels. *Soft Matter* **2016**, *12*, 4300−4308.

(26) Gasser, U.; Weeks, E. R.; Schofield, A.; Pusey, P. N.; Weitz, D. A. Real-Space Imaging of Nucleation and Growth in Colloidal Crystallization. *Science* **2001**, *292*, 258−262.

(27) Auer, S.; Frenkel, D. Prediction of absolute crystal-nucleation rate in hard-sphere colloids. *Nature* **2001**, *409*, 1020.

(28) Lu, P. J.; et al. Orders-of-magnitude performance increases in GPU-accelerated correlation of images from the International Space Station. *J. Real-Time Image Process.* **2009**, *5*, 179−193.

(29) Klein, S. M.; Manoharan, V. N.; Pine, D. J.; Lange, F. F. Preparation of monodisperse PMMA microspheres in nonpolar solvents by dispersion polymerization with a macromonomeric stabilizer. *Colloid Polym. Sci.* **2003**, *282*, 7−13.

(30) Elsesser, M. T.; Hollingsworth, A. D. Revisiting the Synthesis of a Well-Known Comb-Graft Copolymer Stabilizer and Its Application to the Dispersion Polymerization of Poly(methyl methacrylate) in Organic Media. *Langmuir* **2010**, *26*, 17989−17996.

(31) Palangetic, L.; Feldman, K.; Schaller, R.; Kalt, R.; Caseri, W. R.; Vermant, J. From near hard spheres to colloidal surfboards. *Faraday Discuss.* **2016**, *191*, 325−349.

(32) Kaufman, L. J.; Weitz, D. A. Direct imaging of repulsive and attractive colloidal glasses. *J. Chem. Phys.* **2006**, *125*, 074716.

(33) Goff, J.; Arkles, B.; Olenick, L.; Kimble, E. Silicone elastomers by step-growth polymerization of monodisperse dual functional silicones. *Polymer Preprint.* **2012**, *53*, 486.

(34) Kogan, M.; Dibble, C. J.; Rogers, R. E.; Solomon, M. J. Viscous solvent colloidal system for direct visualization of suspension structure, dynamics and rheology. *J. Colloid Interface Sci.* **2008**, *318*, 252−263.

DOI: 10.1021/acs.langmuir.7b00852
Langmuir 2017, 33, 6382−6389

(35) Campbell, A. I.; Bartlett, P. Fluorescent Hard-Sphere Polymer Colloids for Confocal Microscopy. *J. Colloid Interface Sci.* **2002**, *256*, 325−330.
(36) Jardine, R. S.; Bartlett, P. Synthesis of non-aqueous fluorescent hard-sphere polymer colloids. *Colloids Surf., A* **2002**, *211*, 127−132.
(37) Jung, M. E.; Kim, W.-J. Practical syntheses of dyes for difference gel electrophoresis. *Bioorg. Med. Chem.* **2006**, *14*, 92−97.
(38) Kvach, M. V.; Ustinov, A. V.; Stepanova, I. A.; Malakhov, A. D.; Skorobogatyi, M. V.; Shmanai, V. V.; Korshun, V. A. A Convenient Synthesis of Cyanine Dyes: Reagents for the Labeling of Biomolecules. *Eur. J. Org. Chem.* **2008**, 2107−2117.
(39) Mujumdar, R. B.; Ernst, L. A.; Mujumdar, S. R.; Lewis, C. J.; Waggoner, A. S. Cyanine dye labeling reagents: Sulfoindocyanine succinimidyl esters. *Bioconjugate Chem.* **1993**, *4*, 105−111.
(40) Pusey, P. N. The effect of polydispersity on the crystallization of hard spherical colloids. *J. Phys.* **1987**, *48*, 709−712.
(41) Lu, P. J.; Giavazzi, F.; Angelini, T. E.; Zaccarelli, E.; Jargstorff, F.; Schofield, A. B.; Wilking, J. N.; Romanowsky, M. B.; Weitz, D. A.; Cerbino, R. Characterizing concentrated, multiply scattering, and actively driven fluorescent systems with confocal differential dynamic microscopy. *Phys. Rev. Lett.* **2012**, *108*, 218103.
(42) Shen, M. C.; Tobolsky, A. V. Glass Transition Temperature of Polymers. In *Advances in Chemistry*; American Chemical Society, 1965; pp 27−34.
(43) Lesikar, A. V. On the glass transition in organic halide−alcohol mixtures. *J. Chem. Phys.* **1975**, *63*, 2297.
(44) Jenckel, E.; Heusch, R. Die Erniedrigung der Einfriertemperatur organischer Gläser durch Lösungsmittel. *Kolloid-Z.* **1953**, *130*, 89−105.
(45) Xia, Y.; Whitesides, G. M. Soft Lithography. *Angew. Chem., Int. Ed.* **1998**, *37*, 550−575.
(46) McDonald, J. C.; Whitesides, G. M. Poly(dimethylsiloxane) as a Material for Fabricating Microfluidic Devices. *Acc. Chem. Res.* **2002**, *35*, 491−499.

DOI: 10.1021/acs.langmuir.7b00852
Langmuir 2017, 33, 6382−6389